Environmental Pollution 397 (2026) 127904

Contents lists available at ScienceDirect

Environmental Pollution

journal homepage: www.elsevier.com/locate/envpol

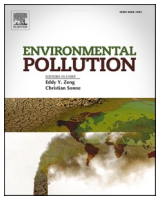

Unveiling the hidden entry route: permeation and accumulation of polycyclic aromatic hydrocarbons through buccal and sublingual mucosa

Cecilia La Mantia [a,1], Giulia Di Prima [b,1], Desirèe Greco [b], Rosalia Ferreri [c], Giuseppina Campisi [d], Fabio D'Agostino [c], Viviana De Caro [b,*]

[a] Department of Precision Medicine in Medical, Surgical and Critical Care (Me. Pre. C.C.), University of Palermo, Via Liborio Giuffrè 5, 90127, Palermo, Italy
[b] Department of Biological, Chemical and Pharmaceutical Sciences and Technologies (STEBICEF), University of Palermo, Via Archirafi 32, 90123, Palermo, Italy
[c] National Council of Research, Institute for Anthropic Impacts and Sustainability in the Marine Environment (CNR-IAS), Via Del Mare N. 3, Torretta Granitola, 91021, Trapani, Italy
[d] Department of Biomedicine, Neurosciences and Advanced Diagnostics (Bi.N.D.), University of Palermo, Via del Vespro 129, 90127, Palermo, Italy

ARTICLE INFO

Keywords:
Phenanthrene
Pyrene
Benzo(a)Pyrene
Oromucosal absorption
PAHs solubility

ABSTRACT

Polycyclic Aromatic Hydrocarbons (PAHs) are persistent and toxic organic pollutants to which humans are exposed via inhalation, dermal absorption, and ingestion, increasing cancer risk, particularly among smokers and occupationally exposed individuals. This research aims to expand current knowledge by identifying the oral mucosae as an additional gateway for PAHs, owing to their high lipophilicity and the greater permeability of oral mucosae to xenobiotics, a finding that is particularly relevant given the established correlation between tobacco-derived PAHs and oral, head, and neck cancers. Here, ex vivo permeation studies were carefully designed using vertical Franz diffusion cells and porcine buccal and sublingual mucosae, a widely used ex vivo model for permeability studies. Five PAHs congeners were selected as representative of those highlighted from the US EPA as priority control pollutants: fluorene, acenaphthene, phenanthrene, pyrene and benzo(a)pyrene. The studied PAHs were found to permeate the oral mucosae, likely via passive diffusion (permeation $\propto$ logP), suggesting a potential relevant contribution to the overall systemic PAHs burden and thus toxicity, especially for individuals with pronounced oromucosal exposure, such as smokers. Additionally, all PAHs exhibited significant retention in the mucosal tissues, suggesting possible loco-regional toxicity. Specifically, the observed BaP accumulation in the buccal and sublingual mucosae (1781.27 $\pm$ 397.64 and 1338.78 $\pm$ 269.47 ng/cm^2, respectively) may support its correlation with oral cancers. Despite the experimental model not fully mimic the complexity of living system (e.g., enzymatic activity, active transport processes, blood perfusion, real-life exposure scenario), these findings address a major gap in the literature by identifying the oral mucosae as a previously unrecognized entry route for PAHs, a key point since the oral cavity is part of both the gastrointestinal and respiratory systems, already recognized PAHs exposure routes. The evidence reported here provides both a foundation for further multidisciplinary investigations as well as a rationale for developing cosmetic/medical devices aimed at detoxifying the oral cavity from PAHs.

Environmental implication: This study aims to expand knowledge on PAHs permeation and accumulation through oral mucosal tissues. Demonstrating PAHs permeation and accumulation through this route would have major clinical and toxicological implications, including identifying a new exposure route, refining toxicokinetic, elucidating mechanisms linking tobacco-derived PAHs to head and neck carcinogenesis, and guiding preventive interventions to limit oral exposure (e.g., development of PAHs-sequestering cosmetics or medical devices).

1. Introduction

Polycyclic Aromatic Hydrocarbons (PAHs) constitute a broad class of organic compounds comprising over one hundred molecules composed exclusively of two or more fused aromatic rings. Based on the number of rings, PAHs are generally classified as light PAHs (containing up to four

* Corresponding author.
E-mail address: viviana.decaro@unipa.it (V. De Caro).
[1] These authors contributed equally to this work.

https://doi.org/10.1016/j.envpol.2026.127904
Received 18 November 2025; Received in revised form 24 January 2026; Accepted 27 February 2026
Available online 28 February 2026

rings) and heavy PAHs (containing more than four rings) (Lawal, 2017). The molecular structure of PAHs significantly influences a range of physicochemical and biological properties, including environmental persistence, corrosion resistance, photosensitivity, vapor pressure, and physical state at ambient temperature. Most PAHs appear as coloured crystalline solids. These compounds can absorb UV-Vis radiation and emit fluorescence, which allows their detection using UV or fluorescence-based analytical systems. Moreover, an increase in the number of aromatic rings and molecular angularity is associated with enhanced hydrophobicity and electrochemical stability. Structural variations are also important due to the strong correlation between charge density and chemical reactivity (Kim et al., 2013). Given these characteristics, PAHs are classified as persistent organic pollutants (Ontiveros-Cuadras et al., 2019). In particular, high-molecular-weight PAHs are recognized as associated with significant risks to both the environment and the human health. Their pronounced lipophilicity might facilitates their translocation across biological membranes and their entry into the bloodstream, where they can associate with plasma lipoproteins determining toxic effects at both systemic and local levels (Ewa and Danuta, 2016). In general, acute effects resulting from PAHs exposure include nausea, vomiting, diarrhoea, and irritation of the eyes or skin, as well as inflammation in cases of contact with anthracene and naphthalene. Chronic effects are associated with the formation of DNA adducts, leading to a significant incidence of severe respiratory tumours (particularly lung cancer) following occupational exposure among workers in iron and steel foundries and in coal and silicon production (Ewa and Danuta, 2016). Moreover, an increased risk and/or predisposing factors for cardiovascular diseases and Attention Deficit/-Hyperactivity Disorder (ADHD) in children have also been reported (Yang et al., 2021). PAHs are primarily generated through incomplete combustion and pyrolysis (thermal degradation in oxygen-deficient conditions) of organic matter. These compounds are ubiquitous in environmental matrices such as air, water, and soil, originating from both natural and anthropogenic sources – including metabolic activity of plants, algae, and humus-degrading microorganisms; volcanic eruptions; forest fires; open-flame cooking; cigarette smoke; oil spills; municipal wastewater; and industrial processes such as aluminium production and coal tar processing (Bansal and Kim, 2015; Boehm, 1964). As a result, exposure to PAHs affects the general population, with elevated risks reported among smokers and workers with occupational exposure (e.g., firefighters, asphalt workers, traffic police). The exposure pathways to PAHs considered to date are as follows.

- Inhalation, which is particularly significant due to the widespread presence of PAHs in ambient air. This route is especially relevant for smokers, individuals exposed to second-hand smoke, and those near combustion sources (Lao et al., 2018). Firefighters, in particular, experienced PAHs levels far exceeding those found in the general environment. However, these exposures can be substantially reduced using appropriate personal protective equipment, which markedly decreases the potential inhalation of PAHs (Teixeira et al., 2025).
- Dermal absorption, as PAHs can penetrate the skin, diffuse through the dermis, and be either metabolized locally (potentially inducing local toxicity and carcinogenesis) or reach systemic circulation (Luo et al., 2020; Williams-Clayson et al., 2024). Specifically, PAHs have been identified on firefighters' skin even when personal protective equipment is worn, indicating that such equipment can mitigate, but not completely prevent, dermal exposure (Sousa et al., 2022).
- Oral ingestion, primarily through consumption of contaminated food, demonstrating the compounds' ability to be rapidly absorbed in the gastrointestinal tract (Kim et al., 2013).

Given the ubiquity of PAHs leading to several human exposure pathways, nowadays numerous studies focus on remediation and bioremediation strategies aimed at reducing upstream exposure through mitigation approaches designed to decrease the concentration of such pollutants in environmental matrices, e.g., water and sediments. These include enzymatic degradation using metabolizing enzymes (Naveed et al., 2025a; Naveed et al., 2025b) as well as electrochemical systems designed to remediate contaminated marine sediments (Proietto et al., 2024).

Despite some studies on systemic PAHs absorption through inhalation, skin and gastrointestinal tract, no data exist, to the best of our knowledge, regarding oromucosal permeation and/or accumulation, an underexplored exposure route that may be relevant due to the oral cavity's anatomical involvement in both inhalation and ingestion processes. The relevance of oromucosal absorption pathway is demonstrated by the extensive researchers' attention it has garnered over the past two decades in the field of drug delivery (El-Say and Ahmed, 2022). Due to their lipophilic nature, PAHs are likely capable of penetrating the oral mucosa, yet no quantitative assessments of this absorption route are currently available. Compared with healthy skin, the oral cavity mucosa shares a stratified epithelial architecture, including keratinocytes, melanocytes, Merkel cells, and Langerhans cells, which protect against fluid loss, toxins, and microbes. However, notable differences exist: the oral epithelium is generally thinner, with less cell layers and higher basal proliferation than skin. Additionally, while the epidermis is fully keratinized, the oral cavity exhibits regional variation, with keratinized epithelium in the hard palate and gingiva and non-keratinized epithelium in the buccal mucosa to accommodate mechanical demands (Waasdorp et al., 2021). Epithelial permeability is largely determined by lipid content: the skin's ceramide-, fatty acid-, and cholesterol-rich stratum corneum forms a strong barrier against water loss and toxins, while oral epithelia, with lower lipid levels in keratinized regions and lipid-supported protection in non-keratinized regions, provide a more permeable barrier against harmful substances and microbial products (Wertz, 2021). In both skin and oral mucosa, substances seem to cross the barrier primarily via passive diffusion (Squier and Lesch, 1988). Furthermore, the buccal route, via the cheek lining, allows delivery of significantly larger molecules, such as peptides and proteins, compared to transdermal delivery, which is generally limited to molecules below ~350 Da. Overall, the oral mucosa's higher permeability (4 to 4000 times that of the skin) combined with its rich vascularization and lower enzymatic activity, enables rapid systemic absorption while bypassing first-pass hepatic metabolism (Caon et al., 2015).

Additionally, numerous indirect evidence already supports the hypothesis of an interaction between PAHs and the oral mucosa. Indeed, the literature clearly reports about the correlation between tobacco-derived PAHs exposure and presence of PAH-DNA adductions potentially leading to oral, head and neck cancers (Foki et al., 2020; Khariwala et al., 2017; Chen et al., 2022; Besarati et al., 2000).

Given the daily exposure to PAHs among both highly exposed individuals (e.g., smokers and firefighters) and the general population (Teixeira et al., 2025; Martín Santos et al., 2020), it is essential to minimize the potential local and systemic health impacts of these compounds.

Therefore, this study aims to elucidate the actual permeability/accumulation of PAHs upon contact with the most permeable oral mucosae namely buccal and sublingual mucosae by using porcine tissues as valid ex vivo models and Franz diffusion cells as two-compartment open model. The demonstration of PAHs permeation/accumulation would have future significant clinical and toxicological implications, including: i) identification of a previously unrecognized exposure route; ii) revision of toxicokinetic and risk assessment models; iii) elucidation of mechanisms underlying the association between tobacco-related PAHs and head and neck cancers (Foki et al., 2020); iv) development of preventive or protective strategies to limit oral exposure; v) improving public health protection and risk mitigation strategies.

2. Material and methods

2.1. Materials

Standard solutions of Polycyclic Aromatic Hydrocarbons (PAHs) containing respectively Fluorene (FLUO), Acenaphthene (ACE), Phenanthrene (PHEN), Pyrene (PYR), and Benzo(a)Pyrene (BaP) in acetonitrile (ACN) at a concentration of 1000 mg/L were supplied from o2si Smart Solutions® (North Charleston, South Carolina, U.S.A.). Propylene Glycol (PGL) was purchased from A.C.E.F. Spa (Fiorenzuola D'Arda, Piacenza, Italy). Polyethylene Glycol 200 (PEG) was obtained from Thermo Fisher Scientific (Segrate, Milan, Italy). The isotonic solution was prepared by dissolving 9 g of NaCl in 1 L of distilled water. The isotonic solution containing trehalose (5% w/v) was prepared by dissolving 50 g of trehalose and 9 g of NaCl in 1 L of distilled water. The non-enzymatic artificial saliva pH 6.8 was prepared by dissolving 0.126 g of NaCl, 0.937 g of KCl, 0.189 g of KSCN, 0.655 g of KH_2PO_4, 0.200 g of urea, 0.154 g of Na_2SO_4, 0.178 g of NH_4Cl, 0.130 g of $CaCl_2$, and 0.631 g of $NaHCO_3$ in 1 L of HPLC-grade water (Gal et al., 2001). The phosphate buffer saline (PBS) pH 7.4 was prepared by dissolving 1.81 g of $Na_2HPO_4{\cdot}2H_2O$, 0.24 g of KH_2PO_4, 0.20 g of KCl, and 8 g of NaCl in 1 L of HPLC-grade water. All chemicals and solvents used, either HPLC or analytical grade, were purchased from Carlo Erba Reagents S.r.l. (Milan, Italy) and VWR International (Leuven, Belgium). The buccal and sublingual mucosae were kindly provided by "Azienda Agricola Mulinello S. r.l." (Enna, Italy) and derived from animals intended for human consumption. Therefore, their use does not require ethics committee approval. All chemicals used for the histological analyses were purchased from Merck Life Science S.r.l. (Milan, Italy).

2.2. Methods

2.2.1. Solubility studies of PAHs in aqueous media in absence or presence of cosolvents

Solubility tests were performed to update outdated data on PAHs solubility in water and to assess their behaviour in the aqueous media generally used to perform ex vivo permeation studies e.g., PBS pH 7.4 and non-enzymatic artificial saliva pH 6.8. To 1 mL of each solvent, 50 μL of either a FLUO:PHEN mixture in ACN (1000 mg/L standards mixed in the 2:3 v/v ratio) or an ACE:PYR:BaP mixture in ACN (1000 mg/L standards mixed in the 3:1:1 v/v ratio) were added. Mixtures were vortexed (LLG-uniTEXER 1) and shaken overnight at room temperature, protected from light (Shaker PS-M3D Variable Speed/Angle). Subsequently, samples were centrifuged for 10 min at 14000 rpm (Eppendorf centrifuge 5415 C), and the supernatant was filtered (syringe filter; 0.45 μm; PTFE) and analysed by HPLC-DAD and/or HPLC-FLR, as described below. The same tests were conducted in PGL-PBS and PEG-PBS mixtures containing 5, 10, and 20% w/w of the chosen cosolvents and then indicated as PBS-PGL-5, PBS-PGL-10, PBS-PGL-20 and PBS-PEG-5, PBS-PEG-10, PBS-PEG-20, respectively. Each experiment was performed in duplicate and results are reported in terms of concentration (μg/mL) as means ($n=2$) ± standard error (SE).

2.2.2. Preparation and conditioning of porcine oromucosal tissues

The porcine buccal mucosa was obtained from the vestibular area of the retromandibular trigone, while the sublingual mucosa was collected from the ventral surface of the tongue of domestic pigs intended for human consumption, with an average age of 12 months. Both tissues were excised immediately after the animal's sacrifice and transported to the laboratory within 2 h into refrigerated boxes, then washed with isotonic solution, cleaned of any excess tissue, and treated for about 1 h with an isotonic solution containing trehalose 5% (w/v), used as a cryoprotectant. The tissues were then drained and stored at −80 ± 1 °C (Thermo Forma ultra-freezer −86 °C mod. 902, Thermo Scientific, Waltham, MA, USA) for at least two weeks before use. Prior to the ex vivo experiments, the tissues were subjected to thermal shock to facilitate separation of both the buccal and sublingual mucosae from the underlying tissue. Frozen samples were immersed in isotonic solution at 70.0 ± 0.5 °C for 1 min. Buccal or sublingual mucosae were then manually detached from the underlying tissue and stored overnight at 4 °C in isotonic solution. Previous studies have shown that this heat treatment does not affect the permeability or integrity of the oral mucosae (Di Prima et al., 2021; Angellotti et al., 2022).

2.2.3. Permeation studies of PAHs through porcine buccal and sublingual mucosae

The permeation studies were performed using vertical Franz-type diffusion cells, employed as a two-compartment open model. The porcine mucosae were mounted between the two compartments, providing an effective permeation area of 0.636 cm^2. During assembly, the acceptor compartment was filled with 15 mL of PBS-PEG-20 and equilibrated at 37.0 ± 0.5 °C in a thermostatic water bath. Vigorous stirring and brief sonication were applied to remove trapped air bubbles. Appropriate sections of the mucosa were then positioned and the donor compartment placed and filled with distilled water. The assembled cells were further conditioned at 37.0 ± 0.5 °C for 15 min. Subsequently, the donor compartment was emptied and loaded with 1 mL of artificial saliva pH 6.8 containing 50 μL of a PAHs mixture in ACN (prepared by mixing 1000 mg/L standard solutions of FLUO, ACE, PHEN, PYR, and BaP in the 2:4:2:1:1 v/v ratio), and sealed with Parafilm® to minimize solvent evaporation and prevent PAHs volatilization. The system was maintained at 37.0 ± 0.5 °C for 24 h under constant magnetic stirring and protected from light. Aliquots of 400 μL were collected from the acceptor chamber at predetermined time points (hourly up to 6 h, with an additional sampling at 24 h). Each removed volume was immediately replaced with fresh acceptor medium to maintain sink conditions. Samples were analysed by HPLC-FLR, as described below. All experiments were repeated eight times, and results are expressed as means ($n=8$) ± SE. Blank reference samples ($n=3$) were obtained by loading into the donor chamber 1 mL of artificial saliva pH 6.8 supplemented with 50 μL of ACN but in absence of PAHs.

2.2.4. Assessment of PAHs accumulation within porcine buccal and sublingual mucosae

At the end of the permeation experiments, Franz cells were disassembled and the mucosal specimens were carefully removed and rinsed with water to remove any trace of residual PAHs precipitated on the mucosal surface. Each mucosa was then placed into a vial and subjected to two consecutive hot-extraction cycles. Specifically, 2 mL of preheated ACN at 82.0 ± 0.5 °C were inserted into the mucosa-containing vial which was sealed with a screw cap fitted with Teflon-lined septa. The mixture was kept at 82.0 ± 0.5 °C for 2 min and then left to cool at room temperature in the dark. Subsequently the extraction liquor was collected and transferred into a 5 mL amber volumetric flask, while the mucosa was subjected to a further extraction cycle with additional 2 mL of ACN. Finally, the collected liquors were brought to volume with the same solvent, and subsequently analysed by HPLC-DAD, as described below. All experiments were repeated five times, and results are expressed as means ($n=5$) ± SE. Blank reference samples ($n=3$) were obtained by subjecting to the extraction procedure the mucosae coming from the permeation assays conducted in absence of PAHs.

2.2.5. Determination of biopharmaceutical parameters: J_s, K_p, t_{lag}, PAH_r and Ac

Mathematical elaboration of the data obtained from the ex vivo studies enabled the evaluation of the following biopharmaceutical parameters: PAHs flux across the buccal and sublingual mucosae (J_s), permeability coefficient (K_p), lag time (t_{lag}), PAHs retention per unit surface area (PAH_r), and accumulation constant (Ac) (Di Prima et al., 2021).

The steady-state flux (J_s) for each PAH was calculated using the following equation:

$$J_s = \frac{Q}{A \times t} \quad \left(\frac{ng}{cm^2 \times h}\right)$$

where Q is the amount (ng) of permeated pollutant over the time interval t (h), and A is the mucosal surface area exposed to PAHs (0.636 cm^2). At the steady state, J_s corresponds to the slope of the linear portion of the curve obtained by plotting the amount of each pollutant permeated per unit surface area (ng/cm^2) versus time (h).

K_p was then obtained as follows:

$$K_p = \frac{J_s}{C_d} \quad \left(\frac{cm}{h}\right)$$

where C_d represents the initial concentration of each pollutant in the donor compartment, which remained constant during the experiment as it reflects the compound's equilibrium solubility in artificial saliva pH 6.8. Indeed, the study design involved the loading into the donor chamber of an excess of PAHs which precipitate on the mucosal surface ensuring saturation conditions over time in order to both maintain the sink conditions until 24 h as well as being consistent with the in vivo exposure circumstances.

The t_{lag} was estimated by extrapolating the x-intercept from the linear portion of the permeation profile.

The amount of PAHs retained within the mucosae per unit area (PAH_r) at the end of each experiment (24 h) was calculated as follows:

$$PAH_r = \frac{Q_T}{A} \quad \left(\frac{ng}{cm^2}\right)$$

where Q_T is the total amount of each pollutant extracted from the mucosa at 24 h.

The Ac was then calculated using the following equation:

$$Ac = \frac{PAH_r}{C_d} \quad (cm)$$

All results are reported as means (n=5) ± SE.

2.2.6. Histological analysis

At the end of the permeation experiments, Franz cells were disassembled and the mucosal specimens were carefully removed and rinsed with water to remove any trace of residual PAHs precipitated on the mucosal surface. Each mucosa was then preserved for microscopic analysis by traditional histology. Three buccal and three sublingual mucosae were preserved in 4% buffered formalin for traditional histological processing. Thus, the tissues were dehydrated using different ethanol concentrations (i.e., 70%, 96%, and 100%) and toluene (EMSURE® ACS, ISO). Embedding process was made by Paraplast, composed of highly purified paraffin-containing plastic polymers of regulated molecular weights (Basilone et al., 2018). Slied (thickness 4 μm) preparation for staining involved xylene (ACS REAGENT ≥98.5%) and ethanol. Finally, Hemalum (Mayer's hemalum solution; Merck Life Science S.r.l., Milan, Italy) and Eosin (B solution; Merck Life Science S.r.l., Milan, Italy) were employed for staining tissues (Atlante di Istologia GUP). Samples were then observed using a stereomicroscope (LEICA DM2500), connected to a camera (LEICA Flexacam C5).

2.2.7. PAHs quantitative analysis

2.2.7.1. HPLC-DAD analysis. HPLC-DAD analyses were carried out using an Agilent 1260 Infinity II system (Agilent Technologies, Santa Clara, CA, USA), equipped with a G1311C quaternary pump, a G7129C autosampler with integrated column thermostat, a 1260 Infinity II G7117C Diode Array Detector (DAD), and interfaced with a computer via the OpenLAB ChemStation 3D UV Workstation (Santa Clara, CA, USA). Chromatographic separation of samples containing the five PAHs was optimized using a reversed-phase Ace® Excel Super C18 column (5 μm, 100 Å, 125 × 4.60 mm; VWR International, USA) as the stationary phase. The mobile phase consisted of water and acetonitrile under isocratic conditions (20:80 v/v), at a flow rate of 1.1 mL/min. The column temperature was maintained at 25 ± 1 °C, the injection volume was set at 20 μL, and the DAD monitored signals within the 190-640 nm wavelength range. In order to quantify the five PAHs, eleven standard solutions in ACN containing all five analytes were injected (concentration range: 0.05-20.00 μg/mL), and calibration curves were constructed as reported in Table S1 (See Supplementary Material).

2.2.7.2. HPLC-FLR analysis. HPLC-FLR analyses were carried out using a Shimadzu LC20AD system (Shimadzu Corporation, Kyoto, Japan), equipped with a quadrupole channel pump, a SIL-20AC-HT autosampler, a SPD-M20A Diode Array Detector (DAD), a RF-10A fluorescence detector (FLR) and interfaced with a computer via the LabSolution software. Chromatographic separation of samples containing the five PAHs was optimized using a reversed-phase Hypersil™ Green PAH Columns (5 μm, 120 Å, 250 × 4.60 mm; Thermo Fisher Scientific) as the stationary phase. The mobile phase consisted of water (eluent A) and acetonitrile (eluent B) under gradient condition, going from 5% to 90% of eluent B in a total of 36 min, at a flow rate of 1.0 mL/min. In order to quantify the five PAHs, standard solutions in ACN containing all five analytes were injected (concentration range: 1-200 ng/mL; FLR detector gain 1x; sensitivity: medium; detection frequency: 3.33 Hz), and calibration curves were constructed as reported in Table S2 (See Supplementary Material).

2.2.8. Data analysis

The data are expressed as means ± standard error (SE). All differences were statistically evaluated with Student's t-test (to evaluate the significance of the highlighted differences among two samples: e.g., comparing buccal and sublingual accumulation of the same PAH) or the one-way analysis of variance (ANOVA or F-test; to evaluate the significance of the highlighted differences among the complete set of data: e.g., accumulation of the five PAHs). Data were considered statistically significant when $p < 0.05$.

3. Results and discussion

3.1. Rational of the study

Polycyclic aromatic hydrocarbons (PAHs) are widely recognized as persistent organic pollutants with harmful effects. Nevertheless, only a limited number of studies have investigated their ability to permeate epithelial barriers, and these have focused primarily on the skin (Sousa et al., 2022), the gastrointestinal and respiratory mucosae (Ewa and Danuta, 2016; Lao et al., 2018). However, the oral cavity is anatomically part of both the digestive and respiratory tracts and its surface is covered by a total of ≈200 cm^2 of distinct mucosal types: i) masticatory mucosa (≈25%), located at the level of the gingivae and hard palate, characterised by a keratinized stratified squamous epithelium and therefore exhibiting low permeability; ii) specialised mucosa (≈15%), localised on the dorsal surface of the tongue and characterised by a variable degree of keratinisation, which is unsuitable for xenobiotic absorption; iii) lining mucosa (≈60%), comprising the buccal and sublingual mucosae, which are non-keratinized tissues characterized by variable thickness (≈100–200 μm in the sublingual mucosa and ≈500–800 μm in the buccal mucosa), and permeability. Specifically, the latter sites have lower mechanical resistance and favour xenobiotic penetration and accumulation. After crossing the epithelium, xenobiotics reach the basement membrane, which does not pose a significant barrier due to its high permeability to nutrients and bioactive molecules. This process is further facilitated by the dense capillary network of the lamina propria, which is responsible for systemic distribution of xenobiotics bypassing hepatic first-pass metabolism (Winning and Townsend, 2000; Mazzinelli et al., 2023a; Dawson et al., 2013). Permeation across the buccal and

sublingual mucosae occurs predominantly by passive diffusion through paracellular or transcellular pathways, depending on the physicochemical properties of the compounds, including molecular size and structure, molecular weight, lipophilicity (log P), and degree of ionization, which is strongly influenced by salivary pH (Sabra et al., 2024). Despite the anatomical characteristics of buccal and sublingual mucosae are particularly favourable for the permeation and accumulation of xenobiotics, no information is currently available regarding PAHs capability of penetrating these oral mucosae and/or accumulating within them. However, several indirect evidence suggests that PAHs can interact with and accumulate within oromucosal tissues, and may also diffuse from the oral cavity to adjacent anatomical sites. Indeed, the literature clearly documents a correlation between exposure to tobacco-derived PAHs and the formation of PAH–DNA adducts, which may contribute to the development of oral, head and neck cancers (Foki et al., 2020; Khariwala et al., 2017; Chen et al., 2022; Besarati et al., 2000).

3.1.1. Rational for PAHs selection

Although sixteen PAHs have been identified by the US EPA as priority control pollutants, in this study five compounds were selected and tested, differing in terms of lipophilicity and chemical structure so as to be representative of the group of sixteen. The chosen PAHs and their main characteristics are reported in Table 1.

3.1.2. Rational for ex vivo permeation study design

The assessment of xenobiotics permeability through mucosal tissues involves different in vitro and ex vivo methods which, with their limitations and advantages, can provide the fundamental scientific knowledge as well as the rationale for the further development and optimization of pharmaceutical products to be used in the oral cavity (Macartney et al., 2025; Pinto et al., 2020).

Since drug permeation through the mucosa is the rate-determining step for systemic absorption, in this study, PAHs ability to cross the buccal and sublingual tissues was assessed using vertical Franz type diffusion cells, a well-established two-compartment open model for permeation studies. The parameters to be considered for the design of an accurate permeation test are numerous and related to the different components of the system: donor and acceptor chambers as well as mucosal membrane.

The donor compartment is generally filled with non-enzymatic artificial saliva pH 6.8 to mimic in vivo conditions. However, to reproduce normal exposure conditions to PAHs, it is necessary to evaluate the amount of each pollutant to be loaded into this compartment. PAHs are generally environmentally present in gaseous, semi-volatile, or particulate forms. In particular, PAHs are generally associated with atmospheric particulate matter which, owing to its colloidal dimensions and consequently large specific surface area, enables the adsorption of substantial amounts of PAHs, delivering them to humans as solids (Kelly and Fussell, 2012). It is thus essential to consider the solubility of PAHs in artificial saliva pH 6.8 to ensure the presence of PAHs precipitate throughout the duration of the experiment.

The acceptor compartment is generally filled with PBS pH 7.4 to simulate plasma. The choice of the acceptor fluid, however, should be guided by the solubility of the molecules under investigation, in order to maintain sink conditions. Indeed, the permeation process must not be limited by the poor solubility of the PAHs in the acceptor compartment. For this purpose, the use of cosolvents that maintain a high concentration gradient while preserving membrane integrity are well established in the literature (Sitovs and Mohylyuk, 2024).

Finally, the ex vivo mucosal membrane should closely resemble human tissues. To this aim, rabbit and porcine mucosae are the mainly used. However, rabbit oral mucosae present the major drawback of providing limited amounts of tissue (Sa et al., 2016), whereas porcine oromucosal tissues are characterized by an extended surface, and it is widely recognized that their permeability values are comparable to those observed across human oral mucosa (Mazzinelli et al., 2023a). Consequently, PAHs passage will be evaluated using porcine buccal mucosal specimens obtained from tissue removed from the inner cheek (buccal) or the ventral surface of the tongue (sublingual) of freshly slaughtered domestic pigs (Mazzinelli et al., 2023b). Moreover, the buccal and sublingual mucosae were selected as previously discussed because they are the most permeable mucosae of the oral cavity (non-keratinized epithelium) (Kulkarni et al., 2010a). Specifically, the porcine buccal and sublingual mucosae are widely regarded as a suitable ex vivo model for human oral mucosa due to substantial anatomical, morphological and permeability similarities. Histological comparisons demonstrate non-keratinized stratified squamous epithelia with comparable epithelial thickness and lipid composition, while permeability assays report analogous flux and permeability coefficients for both hydrophilic and lipophilic compounds. However, minor differences in keratinisation patterns and regional microstructure may influence certain permeation outcomes (Sayed, 2024; Itin et al., 2021; Del Consuelo et al., 2005).

Table 1
Selected PAHs and their main characteristics.

PAH	Molecular Formula	MW (Da)	log P	*IARC classification (group nr.)*	*Chemical* Structure
FLUO	$C_{13}H_{10}$	166.22	4.16	3	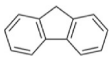
ACE	$C_{12}H_{10}$	154.21	4.19	3	
PHEN	$C_{14}H_{10}$	178.23	4.68	3	
PYR	$C_{16}H_{10}$	202.25	5.17	3	
BaP	$C_{20}H_{12}$	252.31	6.00	1	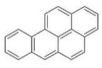

3.2. Preliminary PAHs solubility tests

In view of these considerations, prior to perform the ex vivo permeation assays, PAHs solubility in water, artificial saliva pH 6.8 and PBS pH 7.4 was evaluated. Although conceptually straightforward, the solubility studies posed several challenges. Initial attempts, based on evaporating ACN from PAH standard solutions to obtain solid residues, have been proven to be unsuitable due to light and heat exposure during evaporation, which caused PAHs loss while also leading to the formation of compact residues with limited solid-liquid contact, ultimately resulting in solubility values in water markedly lower than those reported in the literature (Fu and Zou, 2008).

To overcome these limitations, PAH standard solutions in ACN were directly loaded into the studied aqueous media. To minimize ACN cosolvent effects, the water:ACN ratio was kept constant at 1 mL:50 μL. Results are reported in Table 2 and compared with those reported in the literature.

As expected, due to their lipophilic nature, the solubility of PAHs in aqueous media is extremely low. In agreement with the literature (Fu and Zou, 2008), ACE is the most soluble among the PAHs considered. It is interesting to note that, despite the presence of ACN, which may act as a co-solvent, the experimental solubility values in water differ from those reported in the literature, which are found to be two to three times higher. Moreover, significant differences in the experimental results were observed in the presence of salts compared to distilled water. While the composition of the artificial saliva displayed only weak effects on the solubility of most of the studied PAHs, in presence of PBS a marked

Table 2
PAHs solubility in distilled water, non-enzymatic artificial saliva pH 6.8, and PBS pH 7.4, compared to the literature data in terms of water solubility. Means ± SE (*n=2*).

PAH	*Water – literature [Fu and Zou, 2008]*	*Water – experimental*	*Artificial saliva pH 6.8*	*PBS pH 7.4*
		µg/mL		
FLUO	2.000	0.517 ± 0.024	0.508 ± 0.044	0.105 ± 0.008
ACE	3.900	1.328 ± 0.112	1.304 ± 0.135	0.250 ± 0.007
PHEN	1.200	0.641 ± 0.034	0.418 ± 0.021	0.250 ± 0.011
PYR	0.130	0.083 ± 0.007	0.069 ± 0.001	0.104 ± 0.014
BaP	0.004	0.019 ± 0.004	<LOQ	<LOQ

reduction of all the PAHs solubility was observed. In both cases, going from simple distilled water to salts-containing water-solutions lowered the solubility of BaP below the quantification limits. This phenomenon could be due to the salting-out effect, whereby the solubility of an organic compound in water decreases in the presence of dissolved salts. This effect is exploited in salting-out assisted liquid-liquid extraction, where the anions in the aqueous phase enhance phase separation promoting the partitioning of PAHs into the organic solvent (Bressan et al., 2017).

The results obtained allow several important conclusions to be drawn for the accurate design of ex vivo permeation experiments.

- The low solubility of PAHs in artificial saliva pH 6.8 readily enables the preparation of a saturated solution in presence of a PAHs precipitate by employing relatively small amounts of each PAH. This aspect is particularly important considering that the purchased starting PAH stock solutions are in ACN at a standard concentration of 1 mg/mL, as it will prevent the introduction of excessive amounts of ACN into the donor compartment, thereby maintaining the previously tested water:ACN v/v ratio of 1 mL:50 µL.
- The extremely low solubility of PAHs in PBS pH 7.4 prevents its use as acceptor solvent, as it would not ensure the maintenance of sink conditions.

In view of the latter consideration, the use of a cosolvent to be added to PBS in order to obtain a suitable acceptor medium was exploited. The ideal cosolvent should increase PAHs solubilization without interfering with the permeation process (Lane, 2024). Therefore, Propylene Glycol (PGL) and Polyethylene Glycol 200 (PEG200) were tested at three different w/w ratios. Results are reported in Table 3 and highlighted that the presence of cosolvents significantly enhanced PAHs solubility in PBS

Table 3
Solubility of the five PAHs in PBS in presence of PGL and PEG200 as co-solvents employed in the 5, 10, and 20% w/w ratios. Means ± SE (*n=2*).

PAH	Propylene Glycol (PGL)			Polyethylene glycol 200 (PEG200)		
	PBS-PGL-5	PBS-PGL-10	PBS-PGL-20	PBS-PEG-5	PBS-PEG-10	PBS-PEG-20
	µg/mL					
FLUO	0.519 ± 0.030	1.093 ± 0.080	3.110 ± 0.349	0.599 ± 0.011	1.713 ± 0.049	7.846 ± 0.247
ACE	1.301 ± 0.044	2.416 ± 0.102	6.499 ± 0.056	1.476 ± 0.060	3.183 ± 0.023	11.994 ± 0.526
PHEN	0.707 ± 0.030	1.891 ± 0.302	3.931 ± 0.045	0.854 ± 0.022	2.972 ± 0.079	11.348 ± 0.123
PYR	0.117 ± 0.002	0.310 ± 0.005	0.891 ± 0.111	0.171 ± 0.003	0.878 ± 0.012	2.339 ± 0.123
BaP	0.023 ± 0.002	0.050 ± 0.001	0.068 ± 0.004	0.021 ± 0.001	0.062 ± 0.010	0.589 ± 0.024

in a dose-dependent manner. In particular, PEG-solutions showed superior ability to solubilize PAHs when compared to PGL-solutions. Actually, the PBS-PEG-20 mixture solubilises twice the amount of FLUO and ACE, three times the amount of PHEN and PYR, and nine times the amount of BaP compared with the PBS-PGL-20 mixture, overall resulting in an increase in the solubility of FLUO, ACE, PHEN, and PYR in PBS of approximately 75-, 48-, 45-, and 23-fold, respectively. To estimate the increase in BaP solubility – considering that the chromatographic peak observed when evaluating PBS as solvent was below the quantification limit – it is possible to refer to the solubility value reported in the literature for water: this allowed to observe an approximately 150-fold increase in BaP solubility with the PBS-PEG-20 mixture.

3.3. Ex vivo permeation and accumulation studies

3.3.1. Experimental set up

The previously reported results, together with a careful study of the existing literature, allowed the definition of the proper experimental setup for subsequent permeation studies across buccal and sublingual mucosae. Specifically, to maintain sink conditions the chosen acceptor fluid was PBS-PEG-20. Indeed, an apparent increase in the plasma solubility of highly lipophilic and poorly water-soluble molecules can be observed in blood, primarily due to the presence of endogenous components capable of binding, sequestering, or solubilising them, such as plasma proteins, plasma phospholipids, cellular components, and plasma lipoproteins. Specifically, owing to their pronounced lipophilicity, PAHs, once in the bloodstream, tend to associate with plasma lipid fractions rather than remaining dissolved in the aqueous phase. In vitro studies have demonstrated that PAHs, including BaP, are transported in substantial amounts by plasma lipoproteins, with LDL carrying a significant fraction of PAHs mass under equilibrium conditions (National Research Council and United, 1983). Moreover, the use of an acceptor fluid capable of enhancing the solubility of PAHs may also be beneficial in mitigating the limitations associated with the static nature of the Franz vertical diffusion cells. The plasma compartment, in fact, not only presents a volume markedly greater than that of a typical acceptor chamber, but is also characterised by continuous flow, which constantly dilutes the permeated compounds, thereby maximizing the concentration gradient and promoting the permeation process.

A further critical issue for the experimental design is the composition of the donor compartment. To ensure an extremely low amount of ACN (the solvent of PAHs standard solutions) in artificial saliva, so as not to affect membrane permeability, while simultaneously allowing the formation of a saturated solution of PAHs, the donor chamber was filled with 1 mL of artificial saliva pH 6.8 supplemented with 50 µL of a PAHs standard solutions mixture, corresponding to 20 µg of ACE, 10 µg of both FLUO and PHEN and 5 µg of both PYR and BaP. These values were chosen according to both PAHs solubility in artificial saliva as well as literature data on PAHs salivary concentration in smokers and non-smokers (Martín Santos et al., 2020). Indeed, the objectives were: i) to maintain a constant permeation gradient during the experiment, and ii) to replicate, as closely as possible, real-life exposure scenarios under both standard (e.g., non-smokers) and enhanced (e.g., smokers) conditions. Therefore, to ensure a constant concentration gradient, the donor compartment had to be loaded with each PAH in excess respect its solubility in artificial saliva. This excess, or "reservoir", could maintain a steady donor concentration throughout the experiment, theoretically corresponding to the measured solubility. In Table 4, the amounts (µg) of each PAH loaded into the donor compartment (containing 1 mL of artificial saliva) and the corresponding saturation concentrations in saliva are reported, compared with the reported salivary concentrations of four of the five PAHs in non-smoker and smoker subjects, as documented in the literature (Martín Santos et al., 2020). As observable, the amount (µg) of each PAH introduced into the donor compartment is generally lower than the salivary concentration measured in smokers,

Table 4
μg of each PAH loaded into the donor compartment of the vertical Franz cells and corresponding salivary saturation concentrations, compared to the PAHs salivary concentrations in non-smokers and smokers, as reported in the literature.

		FLUO	ACE	PHEN	PYR	BaP
μg_{DONOR}		10	20	10	5	5
$[\mu g/mL]_{DONOR}$		0.508 ± 0.044	1.304 ± 0.135	0.418 ± 0.021	0.069 ± 0.001	0.019 ± 0.004[a]
[μg/mL] DONOR	**Non-smokers**[b]	5.5	3.4	3.1	2.8	N.E.[c]
	Smokers[b]	33.4	10.3	98.8	15.3	N.E.[c]

[a] as the BaP salivary concentration was not quantifiable, for further mathematical evaluation the BaP aqueous solubility value was considered
[b] [Martín Santos P. et al., 2020]
[c] N.E.: Not Evaluated

yet higher than those observed in non-smokers. Nevertheless, the obtained values are not markedly different from an average of the reported real-life concentrations and can therefore be considered indicative of realistic exposure levels.

3.3.2. *Permeation profiles*

The ex vivo behaviour of the five PAHs was monitored determining their concentration hourly until 6 h and evaluating an additional sample recovered after 24 h. The experiments were not extended beyond 24 h, as the maintenance of sink conditions could not have been ensured, nor could mucosal integrity be preserved, particularly for the thinner sublingual mucosa. Additionally, despite the experimental set up was aimed at preventing pollutants loss, it should be considered that PAHs are temperature-sensitive molecules and thus a very small fraction of them may have decomposed or volatilized during the experiments. Nevertheless, this would at most lead to a slight underestimation of the

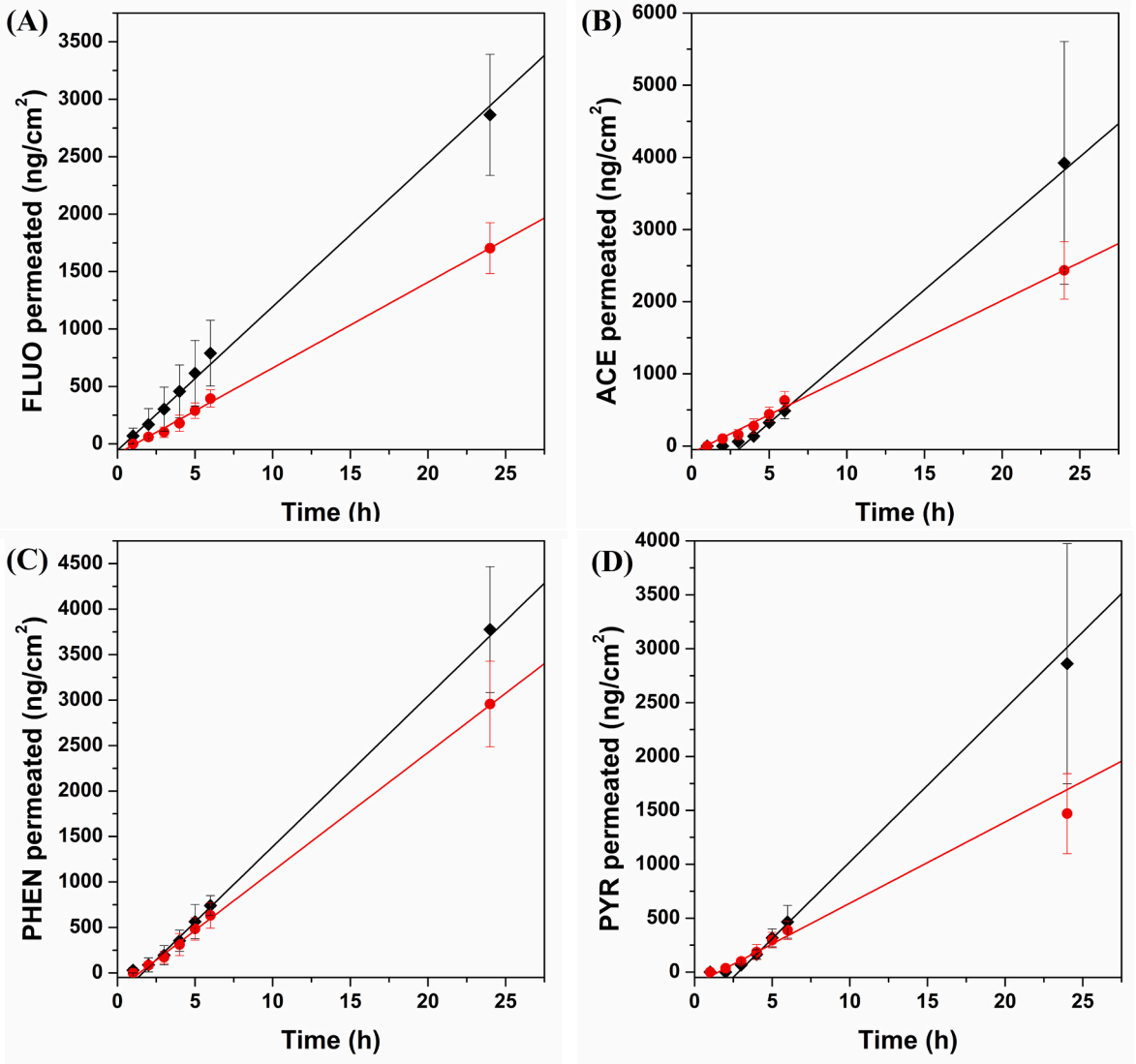

Fig. 1. PAHs permeation profiles: ng/cm^2 of (A) FLUO, (B) ACE, (C) PHEN and (D) PYR permeated through the buccal (black) and sublingual (red) mucosa as a function of time. The linear portions highlighted correspond to the steady-state permeation fluxes. Means ± SE (n=5). (For interpretation of the references to colour in this figure legend, the reader is referred to the Web version of this article.)

measured values and does not compromise the significance of the results. The permeation profiles, reported as ng/cm^2 of each PAH permeated as a function of time, are depicted in Fig. 1, with the exception of BaP, which was undetectable during the first 6 h and was only observed in the 24-h sample. The reported lines represent the flux under steady-state conditions (black line: flux through the buccal mucosa; red line: flux through the sublingual mucosa).

It is noticeable that FLUO, ACE, PHEN and PYR are able to cross the buccal and sublingual mucosae and that the experimental set-up developed was indeed capable of ensuring the maintenance of sink conditions, as the steady-state is generally preserved even when considering the data point corresponding to the 24 h-sampling. To better compare the obtained results, data from the permeation studies were further processed to determine the following biopharmaceutical parameters: J_s (flux), K_p (permeability coefficient), and t_{lag} (lag time to reach the steady state) for each PAH through both buccal and sublingual mucosae, as reported in Table 5.

As observable, the four of five investigated PAHs which were proven to permeate through the oral mucosae exhibited higher fluxes through the buccal mucosa than across the sublingual one. The latter is opposite to the general trend observed when studying xenobiotics oromucosal permeation: usually, higher permeation fluxes are achieved through the sublingual mucosa as it is thinner (100-200 μm) than the buccal one (500-800 μm). However, this apparent discrepancy may be explained by the higher lipophilicity of the buccal mucosa, which promotes stronger interactions of the highly hydrophobic PAHs with the tissue, promoting their penetration and entry into the mucosa as the initial step of permeation. Considering the different solubility of the five PAHs in artificial saliva pH 6.8, and thus their different concentrations into the donor compartment, it is not possible to directly compare J_s values. Comparison in terms of K_p is therefore more meaningful. In particular, K_p resulted inversely proportional to the solubility in saliva and thus the K_p trend was ACE < FLUO < PHEN < PYR. As aqueous solubility increases, PAHs lipophilicity (log P) decreases thus reducing PAH attitude to interact with the lipophilic mucosal tissue and permeate through it. Despite the ex vivo studies allow only a partial discrimination of the mechanistic understanding of the mucosal permeation of the molecules under investigation (e.g., paracellular or transcellular) and do not provide a direct or absolute assessment, the observed relationship between the permeation attitude and the lipophilicity of the considered pollutant could allow some speculations. As more lipophilic molecules exhibited a greater permeation propensity, it can be hypothesised that permeation predominantly occurs via the transcellular route, which is reported in the literature to be favoured for lipophilic and non-ionised molecules, corresponding to PAHs characteristics (Mazzinelli et al., 2023a; Wanasathop et al., 2021; Kokate et al., 2008).

The lag time, defined as the time required to reach steady-state conditions, also provided interesting insights. While lag times were comparable for all PAHs in sublingual mucosa experiments, marked heterogeneity was observed for the buccal mucosa set of experiments. Specifically, FLUO and PHEN, which are both characterized by the presence of a planar bay region in their chemical structures, displayed t_{lag} values significantly lower than those calculated for ACE and PYR. This suggested a correlation between permeation through thicker mucosa and PAHs chemical structures: the presence of more rigid regions within the molecule appears to influence its permeation capacity from a kinetic perspective, promoting a faster interaction with the tissue and, consequently, a more rapid passage through it. Overall, the results demonstrated that PAHs are able to permeate the oral mucosae. The relevance of this finding lies in the identification of a novel hidden entry route for PAHs, which complements established exposure pathways and may contribute to the attainment of toxic systemic concentrations. Although the surface area of the oral cavity with the highest permeability is relatively small (≈120 cm^2) compared to other tissues, such as the skin, the high permeability of these membranes may nevertheless results in a significant increase in the total plasma concentration of PAHs. This may be particularly relevant for at-risk populations, especially those exposed to high local concentrations of PAHs (e.g., smokers).

Table 5
Biopharmaceutical parameters of PAHs: J_s, K_p, and t_{lag}, from the permeation studies across the buccal and sublingual mucosae. Means ± SE (n=5).

		FLUO	ACE	PHEN	PYR	BaP
BUCCAL MUCOSA	J_s (ng/cm^2 • h^{-1})	125.02 ± 4.17	184.33 ± 4.05	165.60 ± 6.97	142.30 ± 6.21	*Null*
	K_p (cm/h)	0.246 ± 0.005	0.141 ± 0.002	0.396 ± 0.010	2.052 ± 0.052	*Null*
	t_{lag}	27 min	3 h 16 min	1 h 37 min	2 h 50 min	*Null*
SUBLINGUAL MUCOSA	J_s (ng/cm^2 • h^{-1})	76.06 ± 3.96	111.13 ± 8.71	130.39 ± 5.63	75.34 ± 5.80	*Null*
	K_p (cm/h)	0.150 ± 0.004	0.085 ± 0.004	0.312 ± 0.008	1.185 ± 0.050	*Null*
	t_{lag}	1 h 19 min	1 h 12 min	1 h 25 min	1 h 36 min	*Null*

3.3.3. Tissue accumulation

Another factor potentially influencing the toxicity is the accumulation of the PAHs within the mucosal tissues. Therefore, at the end of the permeation tests, mucosal samples were subjected to hot extraction in ACN. Fig. 2 shows the amount of each PAH accumulated within buccal and sublingual mucosae, expressed per unit surface area (ng/cm^2).

The high amount of PAHs recovered into the mucosal tissues are certainly coherent with the physicochemical characteristics of the tested molecules. Generally, PAHs are mainly retained from the buccal tissue than the sublingual one and the total amount of PAHs extracted were 8189.1 ± 1367.7 versus 6778.5 ± 1379.9 ng/cm^2, respectively. Again, to better compare the obtained results, data were further processed to determine the following biopharmaceutical parameters: PAH_r (PAHs retention per unit surface area) and Ac (accumulation constant) for each PAH through both buccal and sublingual mucosae, as reported in Table 6.

In this case as well, it is more relevant to compare the obtained results in terms of Ac, as they are normalized to the actual concentration of

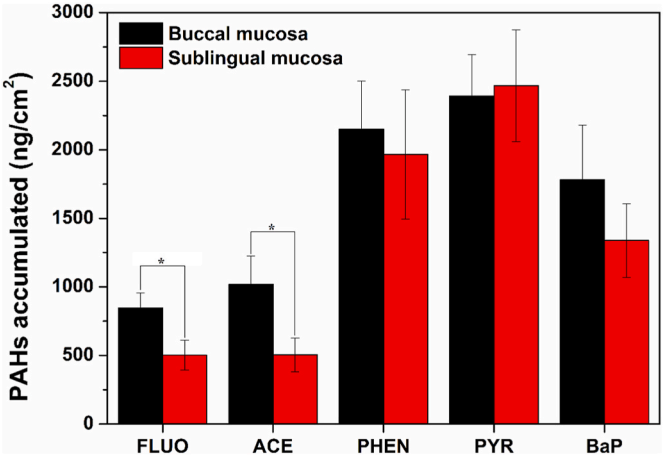

Fig. 2. Amount of FLUO, ACE, PHEN, PYR and BaP (ng/cm^2) accumulated within the buccal (black) and sublingual (red) mucosae at the end of the ex vivo permeation assays. The * indicates a significant difference ($p < 0.05$). Means ± SE (n=5). (For interpretation of the references to colour in this figure legend, the reader is referred to the Web version of this article.)

Table 6
Biopharmaceutical parameters of PAHs: PAH_r and Ac, from the accumulation studies into the buccal and sublingual mucosae. Means ± SE (n = 5).

		FLUO	ACE	PHEN	PYR	BaP
BUCCAL MUCOSA	*PAH_r (ng/cm^2)*	846.33 ± 110.76	1017.66 ± 205.61	2150.90 ± 351.68	2392.94 ± 301.98	1781.27 ± 397.64
	Ac (cm)	1.67 ± 0.13	0.78 ± 0.09	5.15 ± 0.49	34.50 ± 2.51	93.75 ± 12.08[a]
SUBLINGUAL MUCOSA	*PAH_r (ng/cm^2)*	503.04 ± 108.53	504.14 ± 123.17	1964.97 ± 470.90	2467.54 ± 407.84	1338.78 ± 269.47
	Ac (cm)	0.99 ± 0.12	0.39 ± 0.06	4.70 ± 0.65	35.58 ± 3.40	70.46 ± 8.19

[a] Since BaP was not quantifiable in artificial saliva pH 6.8, its aqueous solubility value was considered for a speculative calculation of the Ac.

each PAH into the donor compartment. As previously observed in terms of K_p, again a correlation exists between the PAHs solubility and the Ac value obtained. Specifically, the same trend of inverse proportionality emerged. The retention of PAH resulted in the following tendency: ACE < FLUO < PHEN < PYR < BaP. These results further support the mechanism of permeation previously suggested as generally lipophilic molecules which cross the biomembranes via transcellular route are mainly prone to accumulate within the tissue. It is noteworthy that significant differences were observed for FLUO and ACE, when comparing buccal and sublingual accumulation aptitude. For these two molecules, the Ac values are approximately doubled into the buccal mucosa. This suggests that, for compounds with LogP <4.5, mucosal thickness is a key factor: the thicker buccal mucosa leads to increased accumulation. For compounds with LogP >4.5, extreme lipophilicity appears to outweigh tissue-specific changes, as no significant differences were observed between buccal and sublingual mucosa. Overall, the obtained data suggest high tendency of PAHs to interact with the oromucosal tissues, in accordance with the existing literature which correlated PAHs exposure to PAH-DNA adduct presence in oral cells, potentially contributing to the development of oral, head and neck cancers in humans (Foki et al., 2020; Khariwala et al., 2017; Chen et al., 2022; Besarati et al., 2000).

3.3.4. The case of BaP

BaP, which is the most lipophilic molecule considered (logP = 6.00) as well as the most toxic one, represents an apparently anomalous case. BaP is the only considered PAH that was not detected in the acceptor compartment during the first 6 h of experiment, yet it was quantifiable at the 24 h time point, with values of 21.38 ± 2.01 ng/cm^2 and 72.33 ± 19.22 ng/cm^2 following permeation through the buccal and sublingual mucosa, respectively. These findings are in contrast with the data obtained in terms of the other PAHs permeation: indeed FLUO, ACE, PHEN and PYR exhibited higher permeation through the buccal mucosa respect to the sublingual one. However, it should be considered that BaP has an extremely low solubility in artificial saliva (it was under the LOQ) and thus, once inserted into the donor chamber it might be present almost exclusively as solid. Then it is reasonable that it is not detected for the first 6 h of experiment as the interaction with the tissue, leading to penetration and permeation, can occur only when BaP is molecularly dispersed. Nevertheless, as reported, it was found and quantified into the acceptor chamber at the 24 h-time point as well as it was found into the mucosae at the end of the ex vivo experiments. Given the lipophilic nature of the tissues, it is reasonable to assume that they may gradually "solubilize" BaP, resulting in a prolonged lag time of nearly 24 h.

However, two hypotheses can be formulated regarding the limited permeation observed: i) the solubilization kinetics of BaP could be extremely slow (leading to detection of BaP in the acceptor chamber only in the 24-h sample); ii) BaP high lipophilicity could prevent efficient partitioning from mucosal tissue to the acceptor compartment, determining accumulation in tissues that act as a reservoir, analogous to what occurs in the skin (Zhang et al., 2023). Thus, the higher lipophilicity of the buccal mucosa appears to favour greater accumulation, whereas permeation predominantly occurs through the sublingual tissue, albeit with an extended lag time. This speculative consideration was confirmed by the Ac values obtained. It should be noted that since BaP was not quantifiable in artificial saliva pH 6.8, its aqueous solubility value was considered for a speculative calculation of the Ac. The latter resulted >90 cm and >70 cm for the buccal and sublingual mucosae, respectively. These results support previous hypotheses: BaP has a strong affinity for the thicker and more lipophilic buccal mucosa, where it becomes sequestered, while the thinner sublingual mucosa favours long-term permeation. Overall, BaP's marked accumulation suggests it may exert local toxic effects, especially considering that humans are exposed to BaP from cigarette smoke (20–40 ng/cigarette in smoke of non-filter cigarettes) as well as from indoor and outdoor environmental exposures (e.g., 10.3 μg/m^3 reported by indoor air sampling of emissions from unvented coal combustion) (Chen et al., 2022). The obtained results are consistent with the limited literature on PAHs skin permeability. Alalaiwe et al. (2020) reported increased cutaneous deposition of more lipophilic PAHs, including substantial BaP accumulation (Alalaiwe et al., 2020). Although BaP represents an extreme case, the considerable tissue accumulation of all the five studied PAHs may suggest their potential to induce local toxicity following oromucosal exposure, in accordance with the literature data correlating PAHs exposure to development of oral, head and neck cancers, as previously mentioned.

3.4. Histological studies

Furthermore, to test the inflammatory responses and the occurrence of tissue lesions following ex vivo PAHs treatment, some samples of sublingual and buccal mucosae coming from the permeation studies were not subjected to hot PAHs extraction, yet they were preserved for histological analysis. As observable from the pictures in Fig. 3 (buccal mucosa samples, reported as a representative example), both the PAHs treated (Fig. 3, panel A and C) and the untreated (Fig. 3, panel B and D) tissues appeared without obvious cellular or tissue damage, indicating that they were not symptomatic of inflammatory effects or damage from chemical impact. The slides were analysed considering the usual aspect of both the buccal and the sublingual mucosa, comprising stratified epithelia, containing keratinocytes, melanocytes, Merkel cells and Langerhans cells, which provide protection against body fluid loss, exposure to toxins and microbial invasion (Presland and Jurevic, 2002). The keratinocytes – i.e., the predominant cell population of the epithelium – are arranged in multiple overlapping layers within the oral mucosae. In the deeper layers, the keratinocytes are cuboidal or cylindrical in shape, appearing more compact. In the more superficial layers, they take on a flattened shape and appear slightly dispersed. Other features commonly visible in microscopic analysis of the oral mucosae are the ducts, which are small channels that carry saliva from the salivary glands. These structures were well recognisable in both treated and untreated samples (Fig. 3, panel C and D respectively) and appeared without any signs of damage.

Neither mucosa showed cytological or tissue damage typically associated with accumulation resulting from exposure to PAHs (Boyle et al., 2010). Indeed, accordingly with the literature (Tauchi et al., 2005), the damages most visible through histological analyses – such as increasing collagenous tissue, hypertrophic keratinocytes, or increasing number of Langerhans cells – usually involve prolonged exposure to PAHs and the onset of inflammatory phenomena. As the results confirmed tissue integrity following the described experimental protocol, they also provide evidence that the chosen acceptor medium

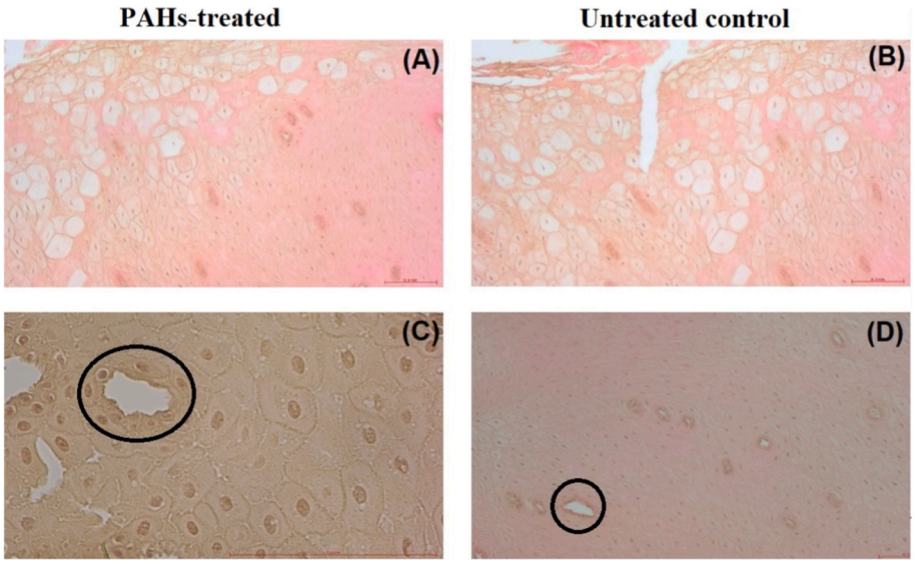

Fig. 3. Slides of the buccal mucosa stained by H&E method following PAHs treatment (panel A magnification: 10×; panel C magnification: 40×) versus untreated control (panel B and D, magnification: 10x). In panel C and D the circles highlight the ducts.

(PBS-PEG-20) does not compromise mucosal integrity or permeability, further supporting its suitability for this study.

4. Study limitations

The ex vivo permeation experiments were conducted using vertical Franz diffusion cells with porcine mucosae as permeation membranes. This experimental setup is widely employed to approximate human oromucosal xenobiotic permeation because of the physiological and anatomical similarities between porcine and human tissues; however, several important limitations must be acknowledged.

First, the static nature of Franz diffusion cells does not replicate the dynamic environment of the oral cavity, including continuous salivary flow and mechanical movements, both of which can significantly influence xenobiotic dissolution and absorption kinetics. Although approaches to simulate salivary washout have been proposed, they remain imperfect representations of in vivo conditions (Mazzinelli et al., 2023a). Moreover, Franz cell experiments do not fully mimic the complexity of living systems, as they generally assume passive diffusion as the primary transport mechanism and neglect enzymatic activity, active transport processes, and blood perfusion, all of which may affect the permeation behaviour of various compounds.

Second, biological variability intrinsic to porcine mucosal tissues (e.g., differences in anatomical site, tissue thickness, handling procedures, storage conditions, and viability) can result in substantial inter-sample variability in permeability measurements, thereby complicating standardization and reproducibility (Kulkarni et al., 2010b). Closely related to this issue, preserving tissue integrity throughout permeation assays is challenging, which limits the feasibility of extending experiments beyond 24 h. Consequently, it was not possible to determine a permeability coefficient (Kp) for BaP, although diffusion into the acceptor compartment was clearly observed. This limitation should be addressed in future investigations.

Finally, inherent differences between porcine and human mucosa, including lipid composition, extracellular matrix organization, and immune features, restrict the direct extrapolation of permeability coefficients and flux data to humans without careful contextualization. Taken together, these considerations highlight the need for complementary experimental models when evaluating oromucosal xenobiotic permeation.

Additional study-specific limitations need to be acknowledged: they are related to the concentrations selected for the donor compartment of the investigated pollutants, owing to the scarce bibliographic data on their actual in vivo salivary levels, both under physiological conditions and in scenarios of increased exposure (e.g., cigarette smoking or occupational settings). All such considerations should be systematically addressed in future studies.

5. Conclusions

The population is continuously exposed to PAHs through inhalation, dermal absorption, and ingestion, as these persistent organic pollutants are ubiquitous in air, water, and soil. Prolonged and repeated exposure poses serious health risks, including chronic inflammation, DNA damage, and an increased incidence of cancer. By applying a sound rationale and carefully selecting the experimental parameters, it was possible to demonstrate that the oromucosal route represents a previously unrecognized pathway of entry for PAHs. This assertion should be interpreted in terms of both systemic entry and loco-regional uptake, with consequent toxic potential affecting the whole organism as well as, more specifically, the treated sites and adjacent areas. With respect to systemic toxicity, BaP may be considered a reference compound, as it is the only established carcinogen among the PAHs investigated in the present study and, owing to its well-documented carcinogenicity, one of the most extensively studied molecules. As an illustrative comparison, the recent study by Beriro et al. (2026) on BaP dermal fluxes following exposure to contaminated soil (BaP concentration: 150 mg/kg) may be considered. Specifically, when comparing the amount of BaP permeated per unit surface area after 24 h through the buccal and sublingual mucosae, the corresponding values are approximately 376- and 1270-fold higher, respectively, than those reported for the dermal route in the literature (0.890, 3.01, and 0.00237 ng/cm^2·h^{-1} for the buccal, sublingual, and dermal routes, respectively) (Beriro et al., 2026). It must certainly be taken into account that the two exposure routes differ markedly in terms of contact surface area, ranging from approximately 1.8 m^2 for the skin to a total of 120 cm^2 for the oral lining mucosae (≈90 cm^2 buccal mucosa; ≈30 cm^2 sublingual mucosa). Assuming static exposure conditions solely for speculative purposes, as they are unrealistic, this would result in a BaP intake of 42.66 ng/h through the skin compared with an intake exceeding 170 ng/h through the oral mucosae. Obviously, as discussed in the limitations section, the oral cavity is subject to continuous salivary wash-out; therefore, it cannot be definitively concluded that oromucosal intake has a greater impact on total exposure than dermal intake. Nevertheless, the relevance of the

oromucosal entry route highlighted herein should be recognized for its contribution to the overall systemic PAHs burden, particularly in individuals with substantial oromucosal exposure, such as smokers. This work has therefore revealed the oromucosal route as an additional gateway for PAHs alongside the already recognized exposure pathways. The results obtained are pioneering and provide valuable stimulus for researchers operating in different fields to further advance knowledge on oromucosal PAHs permeation, for instance through the development of models allowing a more detailed mechanistic understanding.

Regarding the comparison of our data with the tissue accumulation of BaP reported by Beriro et al. (2026), it is possible to observe that the amounts detected in the buccal and sublingual mucosae are respectively 8- and 6-fold higher than those observed at the dermal level (74.20, 55.78, and 8.99 ng/cm^2·h^{-1} for the buccal, sublingual, and dermal routes, respectively) (Beriro et al., 2026). This evidence further correlates high local PAHs exposure events, such as cigarette smoking, with DNA alterations in the affected cells or in immediately adjacent districts, including the formation of PAH-DNA adducts potentially capable of promoting malignant progression, as suggested by the literature.

These findings thus open the way for developing new tools, such as cosmetics and medical devices, to limit or prevent PAHs accumulation through detoxification strategies, which must be carefully designed to ensure consumer safety.

CRediT authorship contribution statement

Cecilia La Mantia: Writing – original draft, Formal analysis, Data curation. **Giulia Di Prima:** Writing – review & editing, Supervision, Methodology, Investigation, Data curation. **Desirèe Greco:** Writing – original draft, Formal analysis. **Rosalia Ferreri:** Investigation, Formal analysis, Data curation. **Giuseppina Campisi:** Writing – review & editing, Resources. **Fabio D'Agostino:** Writing – review & editing, Funding acquisition, Formal analysis, Data curation, Conceptualization. **Viviana De Caro:** Writing – review & editing, Funding acquisition, Data curation, Conceptualization.

Declaration of competing interest

The authors declare the following financial interests/personal relationships which may be considered as potential competing interests: Viviana De Caro reports financial support was provided by Italian Ministry of University and Research (MUR). If there are other authors, they declare that they have no known competing financial interests or personal relationships that could have appeared to influence the work reported in this paper.

Acknowledgement

The project was funded by the National Recovery and Resilience Plan (NRRP), M4.C2.1.1, Call for tender No. 1409 published on September 14, 2022 by the Italian Ministry of University and Research (MUR), funded by the European Union – NextGenerationEU– Project: IPALESS – CUP B53D23031310001- Grant Assignment Decree No. 1369 adopted on September 01,2023 by the MUR.

The authors thank Azienda Agricola Mulinello S.r.l. (EN) Sicilia, for supplying mucosal tissues from pigs and the veterinary Carmelo Giadone for their collection.

The authors thank the Sicily Region that finance PhD scholarships through the project called "Avviso 15/2024 PR FSE + SICILIA 2021/2027 - Finanziamento di borse regionali di dottorato di ricerca in Sicilia A.A. 2024/2025" D.R. 506/2025 PROT. 8615-20/01/2025.

Appendix A. Supplementary data

Supplementary data to this article can be found online at https://doi.org/10.1016/j.envpol.2026.127904.

Data availability

Data will be made available on request.

References

Alalaiwe, A., Lin, Y.K., Lin, C.H., Wang, P.W., Lin, J.Y., Fang, J.Y., 2020. The absorption of polycyclic aromatic hydrocarbons into the skin to elicit cutaneous inflammation: the establishment of structure–permeation and in Silico–in vitro–in vivo relationships. Chemosphere 255. https://doi.org/10.1016/j.chemosphere.2020.126955.

Angellotti, G., Di Prima, G., Scarpaci, A.G., D'Agostino, F., Campisi, G., De Caro, V., 2022. Spray-Dried cytisine-loaded matrices: development of transbuccal sustained-release tablets as a promising tool in smoking cessation therapy. Pharm 2022 14. https://doi.org/10.3390/PHARMACEUTICS14081583, 1583 14, 1583.

Atlante di Istologia GUP. https://gup.unige.it/Atlante-di-Istologia. (Accessed 3 November 2025).

Bansal, V., Kim, K.H., 2015. Review of PAH contamination in food products and their health hazards. Environ. Int. 84, 26–38. https://doi.org/10.1016/J.ENVINT.2015.06.016.

Basilone, G., Gargano, A., Corriero, A., Zupa, R., Santamaria, N., Mangano, S., Ferreri, R., Pulizzi, M., Mazzola, S., Bonanno, A., Passantino, L., 2018. Liver melanomacrophage centres and CYP1A expression as response biomarkers to environmental pollution in European anchovy (Engraulis encrasicolus) from the Western Mediterranean Sea. Mar. Pollut. Bull. 131, 197–204. https://doi.org/10.1016/J.MARPOLBUL.2018.04.028.

Beriro, D., Nathanail, P., Thomas, R., Cocerva, T., Taylor, C., Wragg, J., Lort, J., Williams-Clayson, A., Vane, C., 2026. Application of measured in vitro dermal bioavailability of polycyclic aromatic hydrocarbons (PAH) in soil in detailed quantitative human health risk assessment. Environ. Res. 288, 123176. https://doi.org/10.1016/J.ENVRES.2025.123176.

Besarati, Nia A., Van Straaten, H.W.M., Kleinjans, J.C.S., Van Schooten, F.J., 2000. Immunoperoxidase detection of 4-aminobiphenyl- and polycyclic aromatic hydrocarbons-DNA adducts in induced sputum of smokers and non-smokers. Mutat. Res., Genet. Toxicol. Environ. Mutagen. 468, 125–135. https://doi.org/10.1016/S1383-5718(00)00049-8.

Boehm, P.D., 1964. Polycyclic aromatic hydrocarbons (PAHs). Environ Forensics Contam Specif Guid 313–337. https://doi.org/10.1016/B978-012507751-4/50037-9.

Boyle, J.O., Gümüş, Z.H., Kacker, A., Choksi, V.L., Bocker, J.M., Zhou, X.K., Yantiss, R.K., Hughes, D.B., Du, B., Judson, B.L., Subbaramaiah, K., Dannenberg, A.J., 2010. Effects of cigarette smoke on the human oral mucosal transcriptome. Cancer Prev. Res. 3, 266–278. https://doi.org/10.1158/1940-6207.CAPR-09-0192.

Bressan, L.P., do Nascimento, P.C., Schmidt, M.E.P., Faccin, H., de Machado, L.C., Bohrer, D., 2017. Salting-out assisted liquid-liquid extraction and partial least squares regression to assay low molecular weight polycyclic aromatic hydrocarbons leached from soils and sediments. Spectrochim. Acta Part A Mol Biomol Spectrosc 173, 749–756. https://doi.org/10.1016/j.saa.2016.10.036.

Caon, T., Jin, L., Simões, C.M.O., Norton, R.S., Nicolazzo, J.A., 2015. Enhancing the buccal mucosal delivery of peptide and protein therapeutics. Pharm. Res. 32, 1–21. https://doi.org/10.1007/S11095-014-1485-1/METRICS.

Chen, K.M., Sun, Y.W., Krebs, N.M., Sun, D., Krzeminski, J., Reinhart, L., Gowda, K., Amin, S., Mallery, S., Richie, J.P., El-Bayoumy, K., 2022. Detection of DNA adducts derived from the tobacco carcinogens, benzo[a]pyrene and dibenzo[def,p]chrysene in human oral buccal cells. Carcinogenesis 43, 746–753. https://doi.org/10.1093/CARCIN/BGAC058.

Dawson, D.V., Drake, D.R., Hill, J.R., Brogden, K.A., Fischer, C.L., Wertz, P.W., 2013. Organization, barrier function and antimicrobial lipids of the oral mucosa. Int. J. Cosmet. Sci. 35, 220–223. https://doi.org/10.1111/ICS.12038.

Del Consuelo, I.D., Pizzolato, G.P., Falson, F., Guy, R.H., Jacques, Y., 2005. Evaluation of pig esophageal mucosa as a permeability barrier model for buccal tissue. J. Pharmacol. Sci. 94, 2777–2788. https://doi.org/10.1002/JPS.20409.

Di Prima, G., Angellotti, G., Scarpaci, A.G., Murgia, D., D'agostino, F., Campisi, G., De Caro, V., 2021. Improvement of resveratrol permeation through sublingual mucosa: chemical permeation enhancers versus spray drying technique to obtain fast-disintegrating sublingual mini-tablets. Pharm 2021 13. https://doi.org/10.3390/PHARMACEUTICS13091370. Page 1370 13, 1370.

El-Say, K.M., Ahmed, T.A., 2022. Buccal route of drug delivery. ADME Encycl 222–231. https://doi.org/10.1007/978-3-030-84860-6_12.

Ewa, B., Danuta, M.Ś., 2016. Polycyclic aromatic hydrocarbons and PAH-related DNA adducts. J Appl Genet 2016 583 (58), 321–330. https://doi.org/10.1007/S13353-016-0380-3.

Foki, E., Gangl, K., Kranebitter, V., Niederberger-Leppin, V., Eckl-Dorna, J., Wiebringhaus, R., Thurnher, D., Heiduschka, G., 2020. Early effects of cigarette smoke extract on human oral keratinocytes and carcinogenesis in head and neck squamous cell carcinoma. Head Neck 42, 2348–2354. https://doi.org/10.1002/HED.26247.

Fu, R., Zou, Y., 2008. Analysis of Polynuclear Aromatic Hydrocarbons (PAHs) in Water with ZORBAX Eclipse PAH Column; 5989-7953EN. Agilent Technologies, Shanghai, China, pp. 1–8.

Gal, J.Y., Fovet, Y., Adib-Yadzi, M., 2001. About a synthetic saliva for in vitro studies. Talanta 53, 1103–1115. https://doi.org/10.1016/S0039-9140(00)00618-4.

Itin, C., Domb, A.J., Hoffman, A., 2021. On the suitability of porcine labial mucosa as a model for buccal mucosal drug delivery research. J. Pharmacol. Sci. 110, 1863–1864. https://doi.org/10.1016/j.xphs.2021.01.007.

Kelly, F.J., Fussell, J.C., 2012. Size, source and chemical composition as determinants of toxicity attributable to ambient particulate matter. Atmos. Environ. 60, 504–526. https://doi.org/10.1016/J.ATMOSENV.2012.06.039.

Khariwala, S.S., Ma, B., Ruszczak, C., Carmella, S.G., Lindgren, B., Hatsukami, D.K., Hecht, S.S., Stepanov, I., 2017. High level of tobacco carcinogen-derived DNA damage in oral cells is an independent predictor of Oral/Head and neck cancer risk in smokers. Cancer Prev. Res. 10, 507–513. https://doi.org/10.1158/1940-6207.CAPR-17-0140.

Kim, K.H., Jahan, S.A., Kabir, E., Brown, R.J.C., 2013. A review of airborne polycyclic aromatic hydrocarbons (PAHs) and their human health effects. Environ. Int. 60, 71–80. https://doi.org/10.1016/J.ENVINT.2013.07.019.

Kokate, A., Li, X., Jasti, B., 2008. Effect of drug lipophilicity and ionization on permeability across the buccal mucosa: a technical note. AAPS PharmSciTech 9, 501–504. https://doi.org/10.1208/S12249-008-9071-7.

Kulkarni, U., Mahalingam, R., Pather, I., Li, X., Jasti, B., 2010a. Porcine buccal mucosa as in vitro model: effect of biological and experimental variables. J. Pharmacol. Sci. 99, 1265–1277. https://doi.org/10.1002/jps.21907.

Kulkarni, U., Mahalingam, R., Pather, I., Li, X., Jasti, B., 2010b. Porcine buccal mucosa as in vitro model: effect of biological and experimental variables. J. Pharmacol. Sci. 99, 1265–1277. https://doi.org/10.1002/JPS.21907.

Lane, M.E., 2024. In vitro permeation testing for the evaluation of drug delivery to the skin. Eur. J. Pharmaceut. Sci. 201. https://doi.org/10.1016/j.ejps.2024.106873.

Lao, J.Y., Xie, S.Y., Wu, C.C., Bao, L.J., Tao, S., Zeng, E.Y., 2018. Importance of dermal absorption of polycyclic aromatic hydrocarbons derived from barbecue fumes. Environ. Sci. Technol. 52, 8330–8338. https://doi.org/10.1021/ACS.EST.8B01689.

Lawal, A.T., 2017. Polycyclic aromatic hydrocarbons. A review. Cogent Environ. Sci. 3. https://doi.org/10.1080/23311843.2017.1339841;WGROUP:STRING:PUBLICATION.

Luo, K., Zeng, D., Kang, Y., Lin, X., Sun, N., Li, C., Zhu, M., Chen, Z., Man, Y.B., Li, H., 2020. Dermal bioaccessibility and absorption of polycyclic aromatic hydrocarbons (PAHs) in indoor dust and its implication in risk assessment. Environ. Pollut. 264, 114829. https://doi.org/10.1016/J.ENVPOL.2020.114829.

Macartney, R.A., Das, A., Imaniyyah, A.G., Fricker, A.T.R., Smith, A.M., Fedele, S., Roy, I., Kim, H.W., Lee, D., Knowles, J.C., 2025. In vitro and ex vivo models of the oral mucosa as platforms for the validation of novel drug delivery systems. J. Tissue Eng. 16. https://doi.org/10.1177/20417314241313458. ;PAGE:STRING:ARTICLE/CHAPTER.

Martín Santos, P., Campo, L., Olgiati, L., Polledri, E., del Nogal Sánchez, M., Fustinoni, S., 2020. Development of a method to profile 2- to 4-ring polycyclic aromatic hydrocarbons in saliva samples from smokers and non-smokers by headspace-solid-phase microextraction-gas chromatography-triple quadrupole tandem mass spectrometry. J. Chromatogr. B 1152, 122273. https://doi.org/10.1016/J.JCHROMB.2020.122273.

Mazzinelli, E., Favuzzi, I., Arcovito, A., Castagnola, R., Fratocchi, G., Mordente, A., Nocca, G., 2023a. Oral Mucosa models to evaluate drug permeability. Pharmaceutics 15. https://doi.org/10.3390/PHARMACEUTICS15051559.

Mazzinelli, E., Favuzzi, I., Arcovito, A., Castagnola, R., Fratocchi, G., Mordente, A., Nocca, G., 2023b. Oral Mucosa models to evaluate drug permeability. Pharmaceutics 15. https://doi.org/10.3390/PHARMACEUTICS15051559.

Naveed, M., Saleem, A., Aziz, T., Khatoon, K., Din, M.S.U., Adil, A., Al-harbi, M., Alasmari, A.F., 2025a. Elucidating the synergistic role of hybrid peptide from Burkholderia cepacia enzymes in biodegradation of polycyclic aromatic hydrocarbons. Sci. Rep. 15. https://doi.org/10.1038/S41598-025-97007-1.

Naveed, M., Iqbal, F., Aziz, T., Saleem, A., Javed, T., Afzal, M., Waseem, M., Alharbi, M., Albekairi, T.H., 2025b. Exploration of alcohol dehydrogenase EutG from Bacillus tropicus as an eco-friendly approach for the degradation of polycyclic aromatic compounds. Sci. Rep. 15. https://doi.org/10.1038/S41598-025-86624-5.

Ontiveros-Cuadras, J.F., Ruiz-Fernández, A.C., Sanchez-Cabeza, J.A., Sericano, J., Pérez-Bernal, L.H., Páez-Osuna, F., Dunbar, R.B., Mucciarone, D.A., 2019. Recent history of persistent organic pollutants (PAHs, PCBs, PBDEs) in sediments from a large tropical lake. J. Hazard Mater. 368, 264–273. https://doi.org/10.1016/j.jhazmat.2018.11.010.

Pinto, S., Pintado, M.E., Sarmento, B., 2020. In vivo, ex vivo and in vitro assessment of buccal permeation of drugs from delivery systems. Expet Opin. Drug Deliv. 17, 33–48. https://doi.org/10.1080/17425247.2020.1699913.

Presland, R.B., Jurevic, R.J., 2002. Making sense of the epithelial barrier: what molecular biology and genetics tell Us about the functions of oral mucosal and epidermal tissues. J. Dent. Educ. 66, 564–574. https://doi.org/10.1002/J.0022-0337.2002.66.4.TB03536.X.

Proietto, F., D'Agostino, F., Bonsignore, M., Del Core, M., Sprovieri, M., Galia, A., Scialdone, O., 2024. Electrochemical remediation of synthetic and real marine sediments contaminated by PAHs, Hg and as under low electric field values. Chemosphere 350. https://doi.org/10.1016/j.chemosphere.2023.141009.

Sa, G., Xiong, X., Wu, T., Yang, J., He, S., Zhao, Y., 2016. Histological features of oral epithelium in seven animal species: as a reference for selecting animal models. Eur. J. Pharmaceut. Sci. 81, 10–17. https://doi.org/10.1016/j.ejps.2015.09.019.

Sabra, R., Kirby, D., Chouk, V., Malgorzata, K., Mohammed, A.R., 2024. Buccal absorption of biopharmaceutics classification System III drugs: formulation approaches and mechanistic insights. Pharm 2024 16, 16. https://doi.org/10.3390/PHARMACEUTICS16121563.

Sayed, O.M., 2024. Oral mucosal absorption: mechanisms, methods, and challenges in drug delivery. Int J Clin Med Res 2, 155–170. https://doi.org/10.61466/IJCMR2050002.

Sitovs, A., Mohylyuk, V., 2024. Ex vivo permeability study of poorly soluble drugs across gastrointestinal membranes: acceptor compartment media composition. Drug Discov. Today 29, 104214. https://doi.org/10.1016/J.DRUDIS.2024.104214.

Sousa, G., Teixeira, J., Delerue-Matos, C., Sarmento, B., Morais, S., Wang, X., Rodrigues, F., Oliveira, M., 2022. Exposure to PAHs during firefighting activities: a review on skin levels, in Vitro/In vivo bioavailability, and health risks. Int J Environ Res Public Heal 2022 19 (12677 19), 12677. https://doi.org/10.3390/IJERPH191912677.

Squier, C.A., Lesch, C.A., 1988. Penetration pathways of different compounds through epidermis and oral epithelia. J. Oral Pathol. 17, 512–516. https://doi.org/10.1111/J.1600-0714.1988.TB01326.X.

Tauchi, M., Hida, A., Negishi, T., Katsuoka, F., Noda, S., Mimura, J., Hosoya, T., Yanaka, A., Aburatani, H., Fujii-Kuriyama, Y., Motohashi, H., Yamamoto, M., 2005. Constitutive expression of aryl hydrocarbon receptor in keratinocytes causes inflammatory skin lesions. Mol. Cell Biol. 25, 9360–9368. https://doi.org/10.1128/MCB.25.21.9360-9368.2005.

Teixeira, J., Bessa, M.J., Delerue-Matos, C., Sarmento, B., Santos-Silva, A., Rodrigues, F., Oliveira, M., 2025. Human exposure to polycyclic aromatic hydrocarbons during structure fires: concentrations outside and inside self-contained breathing apparatus and in vitro respiratory toxicity. Environ. Pollut. 373, 126112. https://doi.org/10.1016/J.ENVPOL.2025.126112.

Waasdorp, M., Krom, B.P., Bikker, F.J., van Zuijlen, P.P.M., Niessen, F.B., Gibbs, S., 2021. The bigger picture: why oral mucosa heals better than skin. Biomolecules 11. https://doi.org/10.3390/BIOM11081165.

Wanasathop, A., Patel, P.B., Choi, H.A., Li, S.K., 2021. Permeability of buccal mucosa. Pharm 2021 13, 13. https://doi.org/10.3390/PHARMACEUTICS13111814.

Wertz, P.W., 2021. Roles of lipids in the permeability barriers of skin and oral mucosa. Int. J. Mol. Sci. 22. https://doi.org/10.3390/IJMS22105229.

Williams-Clayson, A.M., Vane, C.H., Jones, M.D., Thomas, R., Taylor, C., Beriro, D.J., 2024. Dermal absorption of high molecular weight parent and alkylated polycyclic aromatic hydrocarbons from manufactured gas plant soils using in vitro assessment. J. Hazard Mater. 469, 133858. https://doi.org/10.1016/J.JHAZMAT.2024.133858.

Winning, T.A., Townsend, G.C., 2000. Oral mucosal embryology and histology. Clin. Dermatol. 18, 499–511. https://doi.org/10.1016/S0738-081X(00)00140-1.

Yang, L., Zhang, H., Zhang, X., Xing, W., Wang, Y., Bai, P., Zhang, L., Hayakawa, K., Toriba, A., Tang, N., 2021. Exposure to atmospheric particulate matter-bound polycyclic aromatic hydrocarbons and their health effects: a review. Int. J. Environ. Res. Publ. Health 18, 1–25. https://doi.org/10.3390/IJERPH18042177.

Zhang, Y., Hu, Q., Fu, J., Li, X., Mao, H., Wang, T., 2023. Influence of exposure pathways on tissue distribution and health impact of polycyclic aromatic hydrocarbon derivatives. Environ. Health (Lond.) 1, 150–167. https://doi.org/10.1021/ENVHEALTH.3C00060.

National Research Council, and United States. Environmental Protection Agency. 1983. *Polycyclic Aromatic Hydrocarbons : Evaluation of Sources and Effects / Committee on Pyrene and Selected Analogues, Board on Toxicology and Environmental Health Hazards, Commission on Life Sciences, National Research Council.* National Academy Press. https://search.library.ucla.edu/discovery/fulldisplay/alma9925150983606533/01UCS_LAL:UCLA. Accessed 23 Jan 2026.